Exploring Therapeutic Potential of Nutraceutical Compounds from Propolis on MAPK1 Protein Using Bioinformatics Approaches as Anti-Coronavirus Disease 2019 (COVID-19)

Khalish Arsy Al Khairy Siregar[1,2], *Paula Mariana* Kustiawan[1*], *Anissa Nofita* Sari[3,2], *Feri Eko* Hermanto[2,4]
[1]Faculty of Pharmacy, Universitas Muhammadiyah Kalimantan Timur, Samarinda, East Borneo 75124, Indonesia
[2]Bioinformatics Research Center, Indonesian Institute of Bioinformatics (INBIO), Malang, Indonesia; 1911102415125@umkt.ac.id (K.A.A.K.S.);
[3]Department of Biochemistry, Medical College of Wisconsin, Milwaukee, Wisconsin, 53226 USA;
[4]Faculty of Animal Sciences, Universitas Brawijaya, Malang, East Java 65145 Indonesia

Abstract. This study explores the potential of propolis, a natural substance, as a gene therapy for treating COVID-19. Despite the advent of COVID-19 vaccines, their side effects pose new health challenges. Utilizing network pharmacology, this research identifies propolis compounds through various databases and assesses their ability to target proteins associated with COVID-19. MAPK1 emerges as a potential therapeutic target, and molecular docking reveals Broussoflavonol F, Glyasperin A, and Sulabiroins as promising compounds with strong binding affinities, i.e., -9.0, -9.0, and -8.8 kcal/mol, respectively, exceeding the native ligand (-7.2 kcal/mol). Molecular Dynamics displays stable complex behavior, with backbone RMSD values consistently below 4 Angstroms and RMSF simulations showing minimal fluctuations within ±2 Angstroms error. Moreover, MM-PBSA analysis further supports the strong binding of Broussoflavonol F, Glyasperin A, and Sulabiroins A, with relative binding energies of -122.82±89.65, 131.48±95.39, and -155.97±111,37 kJ/mol, respectively. These results indicate that propolis has potential as an anti-COVID-19 agent, primarily through inhibiting the MAPK1 pathway. However, further research is needed to validate these results and develop practical applications for COVID-19 therapy. This study underscores the significance of network pharmacology and computational models in understanding propolis mechanisms, offering potential directions for future research and treatment strategies against COVID-19.

1. Introduction

COVID-19, an acute respiratory infectious disease, is attributed to the viral pathogen known as SARS-CoV-2 [1]. Common symptoms of COVID-19 include cough, sore throat, fever,

* Corresponding author : pmk195@umkt.ac.id

arthralgia, myalgia, lethargy, and headache [2]. Patients with comorbidities may experience acute respiratory distress syndrome, shock, metabolic acidosis, and multiple organ failure [3]–[6]. As of November 28, 2022, the global tally of confirmed COVID-19 cases was at 636,440,663, with a corresponding count of 6,606,624 deaths. Despite the development of numerous COVID-19 vaccines and the subsequent initiation of large-scale vaccination campaigns, several vaccines have demonstrated efficacy against SARS-CoV-2 [7]. Although COVID-19 vaccines have been developed and large-scale vaccination campaigns have begun, several vaccines have shown efficacy against SARS-CoV-2. However, the side effects of these vaccines will be a new health problem for humans [8]. These issues encompass thrombocytopenia and vaccine-induced immune thrombosis (VITT), Bell's palsy, and hypersensitivity myocarditis. Hence, investigating genes proves to be a more efficient approach, exhibiting less incidence of adverse effects [9].

Various health interventions have been implemented to mitigate the incidence of COVID-19 infections. These interventions include using masks, adhering to physical distancing measures, practicing proper hand hygiene, and administering vaccines [10]. Herbal medicine constitutes a category of naturally occurring substances employed as adjunctive treatment for COVID-19 [11]. Numerous natural constituents have been documented to possess inhibitory properties against the coronavirus [12]. The antiviral action of Propolis, a resinous substance bees produce, has been documented in scientific literature. This activity is attributed to phenolic chemicals, flavonoids, and aromatic acid esters within Propolis [13]. Propolis has demonstrated inhibitory effects against the varicella-zoster virus, herpes virus, and human immunodeficiency virus, particularly concerning its antiviral action [14]. Preclinical investigations have documented the interactions between Propolis and various target proteins associated with severe acute respiratory syndrome coronavirus 2 (SARS-CoV-2), the causative agent of COVID-19 [15]. Moreover, several clinical investigations have provided evidence regarding the possible beneficial impacts of propolis and honey products on the elimination of the SARS-CoV-2 virus and the alleviation of patient symptoms [10]. Nevertheless, the current body of knowledge regarding prospective biomarkers for COVID-19 remains significantly limited, with a shortage of comprehensive understanding regarding the underlying mechanisms involved [16–18].

The objective of this study was to stimulate an intellectually stimulating discussion on the potential use of Propolis for the management of COVID-19, employing modern advancements in computer-assisted drug design, namely network pharmacology [19]. Network pharmacology is a discipline that falls under systems biology theory, incorporating many approaches like high-throughput omics data analysis, computer virtual computing, and network database retrieval [20]. Systematic biological network analysis is a prevalent strategy in modern-day research [21]. This emerging field of study can forecast potential pharmacological targets from a holistic standpoint, thereby enhancing the efficacy of the drug development procedure. The discipline of network pharmacology has successfully surmounted past challenges associated with single-target, single-drug investigations. It has garnered considerable momentum in the identification of active constituents and comprehension of efficacious approaches [22]. The organization of pharmacological and structural health networks is aligned with the complete qualities of Propolis, which contributes to the advancement of our comprehension of the intricate mechanisms encompassing many ingredients, targets, and pathways in herbal therapy [23-24]. Furthermore, this study examined genetic material derived from publicly available bioinformatics sources. Moreover, molecular docking, a technique based on the fundamental principles of ligand-receptor interactions, is a versatile technology employed to elucidate the mechanisms by which chemical compounds interact with their molecular targets [25-26]. Consequently, it is widely utilized in pharmaceutical research and development. Molecular dynamics (MD) simulations elucidate the dynamic characteristics of biomolecules at the

atomic level, offering a dependable representation of their structural soundness [27]. The present study holds promise for establishing a theoretical framework that can facilitate the development of novel pharmaceutical interventions and elucidate the underlying mechanisms implicated in the pathogenesis of COVID-19. This study employed network pharmacology, molecular docking, and molecular dynamics (MD) modeling methodologies to investigate the active ingredients, molecular targets, and significant biological pathways associated with the anti-COVID-19 capabilities of Propolis.

2. Materials and Methods

2.1 Acquisition of Compounds Database for Propolis compounds

The compound database in propolis was obtained from several previously reported literature [28–36], compounds not in the PubChem database will be visualized using the Marvin JS *plug-in* on the SwissADME Web server (http://www.swissadme.ch/index.php) [37].

2.2 Compounds and COVID- 19 Associated Targets

Identification of the target genes related to the filtered constituents was achieved via accessible online tools such as the STITCH DB (http://stitch.embl.de/), TargetNet (http://targetnet.scbdd.com/), and SwissTargetPrediction (http://www.swisstargetprediction.ch/) with the specification "*Homo Sapiens*" and 'Probability 0.6', which is used as a filter to predict the target protein in [38]–[40]. Furthermore, to find targets related to COVID-19, a search was carried out using the GeneCards Website Database (https://www.genecards.org/) with a cutoff (>2) [41]. The Online Venn Diagram Generator (http://bioinformatics.psb.ugent.be/webtools/Venn/) analyzed the interrelationships between the propolis target protein and the target protein related to COVID-19.

2.3 Enrichment Analysis

The Database for Annotation, Visualization, and Integrated Discovery (DAVID database, https://david.ncifcrf.gov/) was used for enrichment analysis and visualization of Gene Ontology (GO), Biological Process (BP), and KEGG pathways of overlapping Propolis gene targets. The findings of combinations of proteins associated with Propolis and COVID-19 were then filtered using the parameter *P-value* <0.05 to quantify statistical differences and target potential [42]–[44]. The Gene Ontology of Biological Process and KEGG target data were shown using the Bioinformatics website platform (http://www.bioinformatics.com.cn) [45]–[48] and GraphPad Prism 9.0.0.

2.4 Identification of Core Targets of Propolis against for COVID-19

Targets identified using Gene Ontology of Biological Process and KEGG were collected and analyzed using STRING Database Ver.11.5 (https://string-db.org/) network map and .tsv extension data to conduct an in-depth study of protein-protein interaction (PPI) between Propolis and COVID-19 [49], [50]. Topological characteristics were examined using the Network-Analyzer settings of the Cytoscape program [51]. The anticipated target proteins and associated target proteins were excised and examined using Cytoscape software (https://cytoscape.org/, Version 3.7.2) to investigate the pharmacological mechanism of Propolis in COVID-19. The Cytoscape *CytoHubba plugin* was used to investigate protein

interactions. Maximal Clique Centrality (MCC), Density of Maximum Neighborhood Component (DMNC), Maximum Neighborhood Component (MNC), Degree Centrality, Edge Percolated Component (EPC), BottleNeck, EcCentricity, Closeness, Radiality, Betweenness, Stress, and ClusteringConff are among the 12 techniques presented [52]–[54]. After comparing the data, the MAPK1 gene were discovered in 11 of the 12 techniques tested for Molecular Docking Analysis.

2.5 Molecular Docking

The molecular docking procedure was performed with the Autodock Vina algorithm implemented in the PyRx program, version 0.9.9 [55]. The crystal structures of the MAPK1 protein target, specifically the PDB ID: 3SA0 [56], were obtained from the RCSB Protein Data Bank (http://www.rcsb.org/) [57]. The Macromolecules and Propolis compounds were sourced from the PubChem database, accessible at https://pubchem.ncbi.nlm.nih.gov/ [58]. The protein structures were generated with Autodock tools-1.5.7. This process encompassed the elimination of water molecules and heteroatoms, the introduction of hydrogen polar groups, the consolidation of non-polar groups, and the integration of gasteiger charges. The protein structures generated were then stored in a file format referred to as pdqt format. Before initiating molecular docking, the protein structure was confirmed by redocking the co-crystallized ligand within the protein's binding area. The utilization of Autodock Vina, a software utility accessible in PyRx version 0.9.9, facilitated the accomplishment of this task. The selection of binding sites was conducted by utilizing a grid box centered on the ligand for each protein in Autodock. The grid box was built to enclose the protein's active region, MAPK1, utilizing the XYZ coordinates (-14.992, 14.3, and 41.122). The grid was configured with dimensions of 20x20x20. The LigRMSD (https://ligrmsd.appsbio.utalca.cl/) value of 0.74 Å was employed to calculate the root mean square deviation between crystalline ligands before and following re-docking [59]. This deviation must remain confined to the range of 2Å. The process by which a ligand can form a binding interaction with a receptor is widely recognized in scientific literature as affinity. The BIOVIA Discovery Studio Visualizer presents data in a three-dimensional format [60].The LigPlot software was employed to examine the interactions between proteins and ligands in PDB files containing encrypted docking data [61], [62]. The present study involved a comprehensive analysis of three compounds exhibiting superior binding affinity alongside a control consisting of the Native Ligand. These compounds were subjected to rigorous investigation using Molecular Dynamics.

2.6 Molecular Dynamics

The simulations utilized YASARA version 21 software, employing the AMBER14 forcefield [63], [64]. The parameters of the simulation are as follows: The experimental conditions included a pH of 5.0, a NaCl concentration of 0.9%, a water density of 0.997, a pressure of 1 atm, a running time of 20 ns, a temperature of 310°K, and a cubic grid form. The determination of bond energy stability or molecular mechanics energies, in conjunction with the Poisson-Boltzmann (MMPBSA) approach, was performed using the Poisson-Boltzmann (PBS) method [65]. This analysis was conducted on the macros md_analyzebindingenergy.mcr obtained from YASARA [66].

3. Results and Discussion

3.1 Identifying Propolis targets and intersection COVID-19

Comprehensive set of 1438 proteins associated with COVID-19 was acquired from the GeneCards webserver. Additionally, 313 proteins related to Propolis were obtained through STITCH, TargetNet, and Swiss Target Prediction. Subsequently, an intersection analysis was performed, resulting in the identification of 74 proteins that were common to both propolis compounds and COVID-19-related proteins. These findings were visually represented using a Venn diagram (Figure 1).

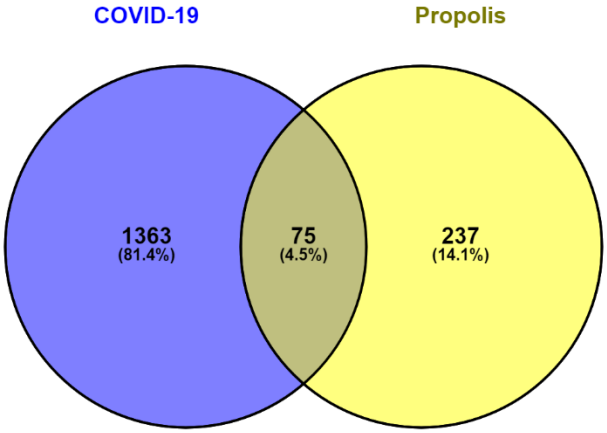

Fig. 1. Venn diagram results, Intersection results between Propolis related genes and COVID-19 Genes.

3.2 Biological Function and Pathway Enrichment Analysis

The biological functions of the 74 probable protein targets were determined using Gene Ontology and KEGG pathway enrichment analysis. In the GO study, 399 GO keywords were discovered, including 62 Molecular Functions (MF), 282 Biological Processes (BP), and 55 Cellular Components (CC), where these data were collected using a *p-value* threshold of (<0.05). The top ten BP words are ordered by *p-value* and the quantity of protein listed (Figure 2). The main GO terms BP are related to protein phosphorylation, response to xenobiotic stimulus, response to drug, peptidyl-serine phosphorylation, positive regulation of gene expression, negative regulation of apoptotic process, positive regulation of neuron apoptotic process, cellular response to reactive oxygen species, peptidyl-threonine phosphorylation, positive regulation of transcription, DNA-templated. Furthermore, the Coronavirus disease - COVID-19 pathway from Propolis is shown by the KEGG pathway enrichment analysis, which is the focus of this research topic, to be significantly associated with 74 potential pathways (Table 1).

Table 1. KEGG Pathways

KEGG Pathway	Count	*P Value*	Genes
Pathways in cancer	25	3.71E-12	GSK3B, HDAC2, PIK3R1, PTGS2, RELA, EGFR, MAPK8, CASP3, ERBB2, AKT1, HMOX1, MAPK1, SMAD2, JUN, HSP90AA1, NOS2,

			MMP1, FOS, F2, IL2, CCNA2, AR, CDK2, PPARG, MET
Lipid and atherosclerosis	15	2.49E-09	GSK3B, JUN, HSP90AA1, NOS3, MMP1, MMP3, PIK3R1, FOS, TNF, RELA, MAPK8, CASP3, AKT1, MAPK1, PPARG
MicroRNAs in cancer	15	2.57E-07	ABCC1, DNMT1, HDAC2, PRKCE, PIK3R1, PTGS2, EGFR, PLAU, CASP3, ERBB2, CYP1B1, HMOX1, MAPK1, MET, MCL1
Apoptosis	14	8.48E-11	JUN, PARP1, BCL2A1, PIK3R1, FOS, TNF, RELA, MAPK8, CASP3, CTSK, AKT1, MAPK1, CTSB, MCL1
Human T-cell leukemia virus 1 infection	14	3.56E-08	SMAD2, JUN, PIK3R1, FOS, TNF, IL2, RELA, CCNA2, MAPK8, LCK, CHEK2, CDK2, AKT1, MAPK1
Chemical carcinogenesis - reactive oxygen species	14	3.75E-08	PTPN1, JUN, AKR1A1, AHR, PIK3R1, FOS, EGFR, RELA, MAPK8, CYP1B1, AKT1, HMOX1, MAPK1, MET
PI3K-Akt signaling pathway	14	7.33E-06	GSK3B, HSP90AA1, NOS3, PIK3R1, EGFR, IL2, PIK3CG, RELA, ERBB2, CDK2, AKT1, MAPK1, MET, MCL1
Alzheimer disease	14	1.76E-05	GSK3B, APP, NOS2, CSNK2A1, PIK3R1, PTGS2, TNF, RELA, BACE1, MAPK8, CDK5, CASP3, AKT1, MAPK1
IL-17 signaling pathway	13	1.54E-11	GSK3B, JUN, HSP90AA1, CCL11, MMP1, MMP3, FOS, PTGS2, TNF, RELA, MAPK8, CASP3, MAPK1
Chagas disease	13	4.12E-11	SMAD2, JUN, NOS2, SERPINE1, PIK3R1, FOS, TNF, IL2, RELA, MAPK8, TLR9, AKT1, MAPK1
Prostate cancer	12	4.31E-10	GSK3B, AR, HSP90AA1, PLAU, ERBB2, CDK2, MMP3, MAPK1, AKT1, PIK3R1, RELA, EGFR
AGE-RAGE signaling pathway in diabetic complications	12	6.01E-10	SMAD2, JUN, MAPK8, NOS3, CASP3, PRKCE, SERPINE1, MAPK1, AKT1, PIK3R1, TNF, RELA
Relaxin signaling pathway	12	9.30E-09	SMAD2, JUN, MAPK8, NOS2, MMP1, NOS3, MAPK1, AKT1, FOS, PIK3R1, RELA, EGFR
Measles	12	2.04E-08	GSK3B, JUN, MAPK8, CSNK2A1, CASP3, CDK2, TLR9, AKT1, FOS, PIK3R1, RELA, IL2
Coronavirus disease - COVID-19	12	3.62E-06	JUN, MAPK8, MMP1, MMP3, MAPK1, FOS, PIK3R1, F2, TNF, RELA, EGFR, IL2

Human papillomavirus infection	12	9.98E-05	CCNA2, GSK3B, HDAC2, CASP3, CDK2, MAPK1, AKT1, PIK3R1, PTGS2, TNF, RELA, EGFR
Pathways of neurodegeneration - multiple diseases	12	0.002144011	GSK3B, APP, MAPK8, CSNK2A1, NOS2, CDK5, CASP3, SIGMAR1, MAPK1, PTGS2, TNF, RELA
T cell receptor signaling pathway	11	1.46E-08	GSK3B, JUN, MAPK8, LCK, MAPK1, AKT1, FOS, PIK3R1, TNF, RELA, IL2
TNF signaling pathway	11	2.99E-08	JUN, MAPK8, CASP3, MMP3, MAPK1, AKT1, FOS, PIK3R1, PTGS2, TNF, RELA
Osteoclast differentiation	11	1.08E-07	JUN, MAPK8, LCK, CTSK, MAPK1, AKT1, PPARG, FOS, PIK3R1, TNF, RELA

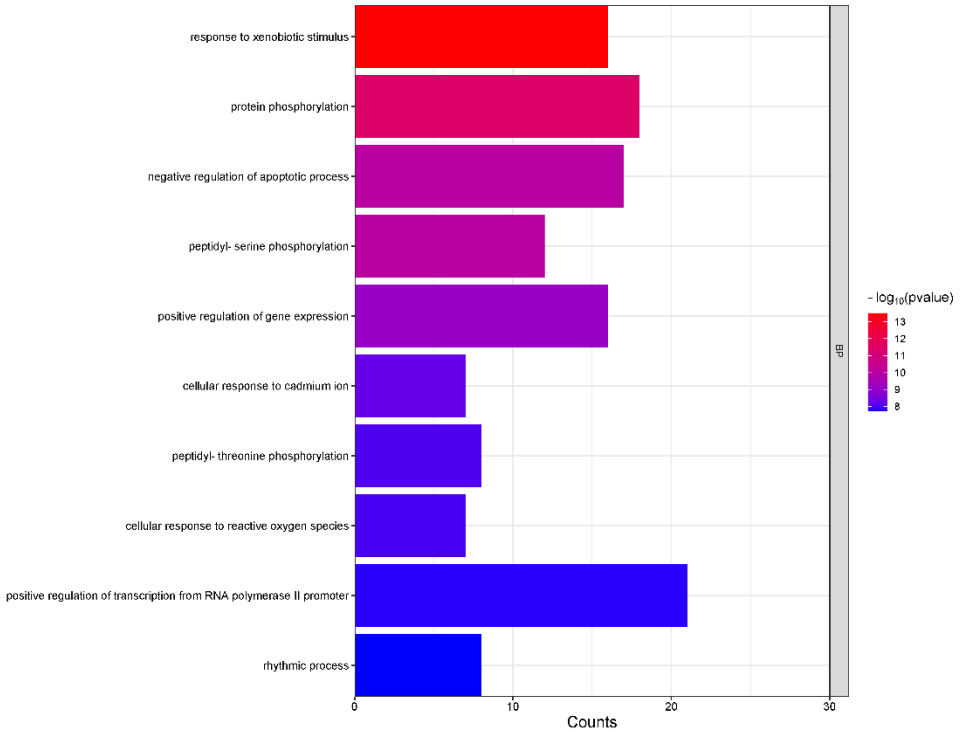

Fig. 2. Biological Process Results.

3.3 Components-Targets Network Construction of COVID-19

To determine a protein's crucial involvement in COVID-19, proteins from the Top 10 GO BP and 20 KEGG were gathered, and up to 26 proteins were evaluated using STRING analysis and protein network topology. The interactive protein-related protein from Propolis to COVID-19 was assessed with the Tool Cytoscape program and the *CytoHubba plug-in*, with at least two *CytoHubba* techniques used as a cutoff in this procedure. Table 2 shows that the twelve *CytoHubba* techniques contain a total of 19 proteins. Among the 19 proteins, MAPK1 is at the top with its appearance in eleven different methods: Betweenness Method, Stress Method, Degree Method, EPC, Closeness Method, Radiality Method, MCC Method,

BottleNeck Method, MNC Method, EcCentrality Method, and DMNC Method. In addition, AKT1, JUN, and RELA were present in ten methods, HSP90AA1 and LCK were present in nine methods, IL2 in eight methods, EGFR and PIK3R1 in seven methods, MAPK8 in six methods, APP in four methods, CASP3, CDK1, and FOS in three methods, and last AR, NOS2, PRKCE, PTPN1, and TNF proteins were present in only two methods. To see this in Figure 3. is a visual representational proof for the occurrence of screened genes in the various *CytoHubba* methods.

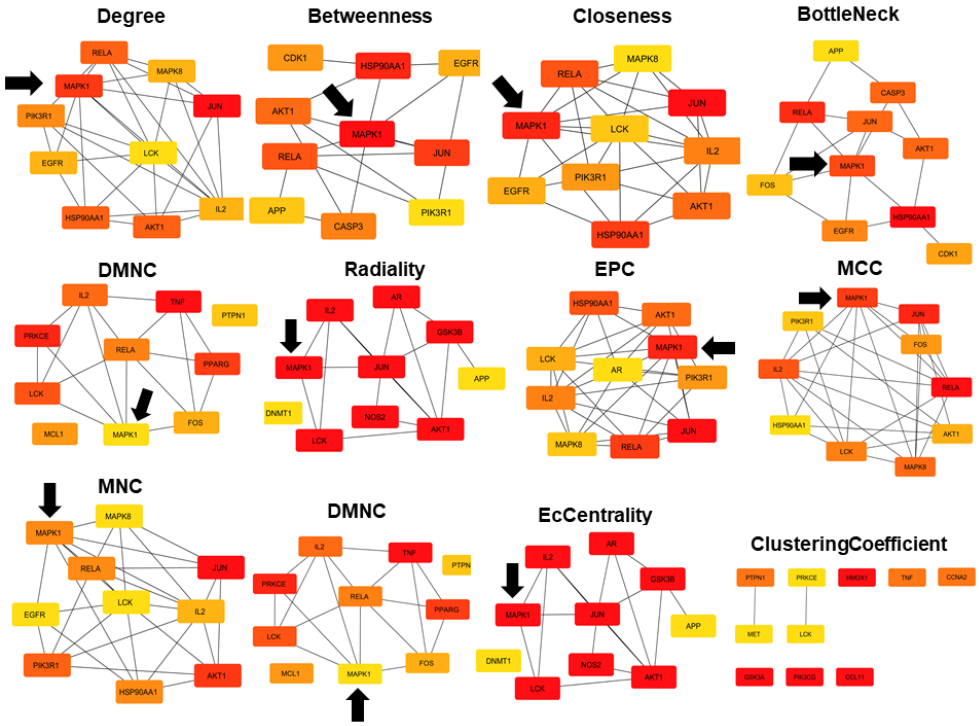

Fig. 3. The presence of filtered genes in all twelve CytoHubba techniques, with MAPK 1 present in eleven (Betweenness, Stress, Degree, EPC, Closeness, Radiality, MCC, BottleNeck, MNC, EcCentrality, and DMNC)

Table 2. List of the genes present from twelve different methods of the CytoHubba plugin Cytoscape

Genes	Occurrences	Present In (Methods)
MAPK1	11	Betweenness, Stress, Degree, EPC, Closeness, Radiality, MCC, BottleNeck, MNC, EcCentrality, DMNC
AKT1	10	MNC, Degree, EPC, BottleNeck, EcCentrality, Closeness, Radiality, Betweenness, MCC
JUN	10	MNC, Degree, EPC, EcCentrality, Closeness, Radiality, MCC, Betweenness, Stress, BottleNeck
RELA	10	MCC, BottleNeck, EPC, Degree, Closeness, Radiality, Betweenness, Stress, MNC, DMNC
HSP90AA1	9	BottleNeck, Betweenness, Stress, Closeness, Radiality, MNC, EPC, Degree, MCC
LCK	9	DMNC, MCC, EcCentrality, Radiality, MNC, EPC, ClusteringCoefficient, Closeness, Degree

IL2	8	MCC, DMNC, EPC, Closeness, Radiality, MNC, EcCentrality, Degree
EGFR	7	BottleNeck, Stress, Degree, Closeness, Radiality, Betweenness, MNC
PIK3R1	7	MNC, Degree, EPC, Closeness, MCC, Stress, Betweenness
MAPK8	6	MNC, Degree, EPC, MNC, Closeness, Radiality
APP	4	EcCentrality, Betweenness, BottleNeck, Stress
CASP3	3	BottleNeck, Betweenness, Stress
CDK1	3	Betweenness, BottleNeck, Stress
FOS	3	MCC, DMNC, BottleNeck
AR	2	EPC, Ec Centrality
NOS2	2	EcCentricity, Radiality
PRKCE	2	ClusteringCoefficient, DMNC
PTPN1	2	ClusteringCoefficient, DMNC
TNF	2	DMNC, ClusteringCoefficient

3.4 Molecular Docking Results

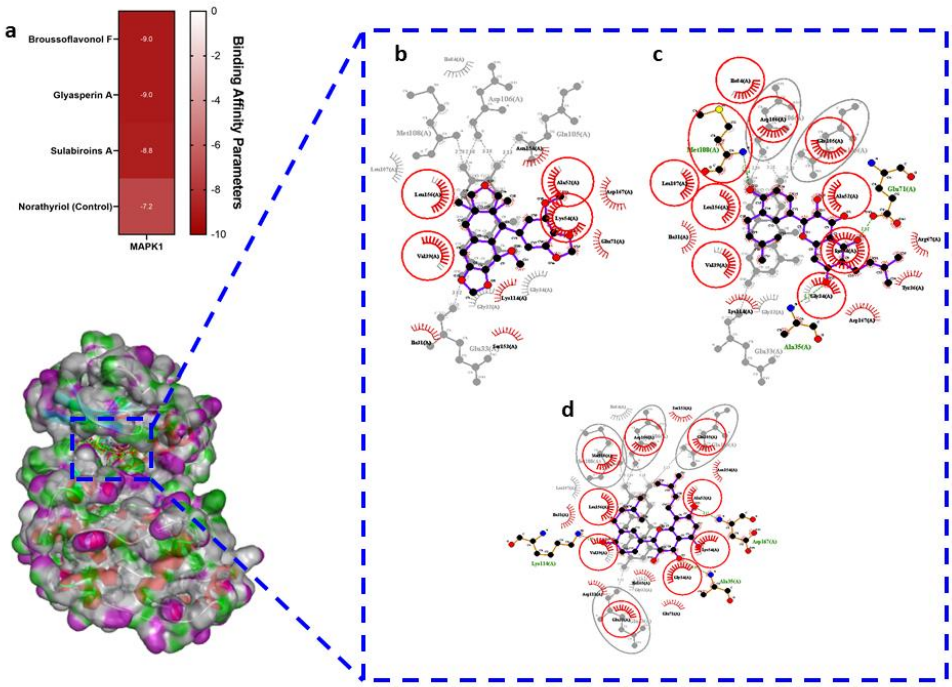

Fig. 4. Docking Result in LigPlot+ Visualization (a) Heatmap Docking Results, (b) Broussoflavonol F, (c) Glyasperin A and (d) Sulabiroins A.

We used VinaWizard algorithm in the PyRx software version 0.9.9 to perform molecular docking to validate further the binding affinity of the propolis compound and MAPK1 protein, where Norathyriol is the Native Ligand in MAPK1. Based on the results of docking, where Norathyriol, which acts as a Native Ligand, has a docking score (-7.2 kcal/mol).

Meanwhile, out of a total of 21 propolis compounds, three compounds had the highest binding affinity, namely Broussoflavonol F (-9 kcal/mol), Glyasperin A (-9 kcal/mol), and Sulabiroins A (-8.8 kcal/mol). To see the bonds inside, Native Ligand (Norathyriol) forms 4 (Glu33, Met108, Asp106, and Gln105) Hydrogen Bonds and 8 (Gly32, Val39, Gly34, Lys54, Leu156, Ala52, Leu107, and Ile84) Hydrophobic Interaction. Then in the three compounds with the highest Binding Affinity, Broussoflavonol F forms 3(Asp167, Ala35, and Lys114) Hydrogen Bonds, 15(Ile165, Leu156, Gln105, Met108, Val39, Asp106, Ile31, Ala52, Asp111, Ser153, Glu33, Gly34, Glu71, Lys54, and Asn154) Hydrophobic Interaction, Glyasperin A triple (Ala35, Glu71, and Met108) Hydrogen Bond and 14 (Tyr36, Arg67, Lys54, Leu156, Ile84, Asp106, Ala52, Leu107, Gln105, Ile31, Lys114, Gly34, Val39, and Asp167) Hydrophobic Interaction. Finally, the Sulabiroins A compound has 10 (Glu71, Asp167, Ser153, Asn154, Leu156, Val39, Ala52, Ile31, Lys114, and Lys54) Hydrophobic Interaction. Based on the literature from the PDB source, it is stated that the residues Gln105, Asp106, and Met108 are the active sites for the bond with the Native Ligand (norathyriol) [56]. This is directly proportional to the results obtained for the compounds Broussoflavonol F and Glyasperin A. Twentyone docked propolis compounds were selected for the top three propolis compounds based on their binding affinity score will conducted Molecular Dynamics to evaluate RMSD, RMSF, and binding energy calculation along simulation 20ns.

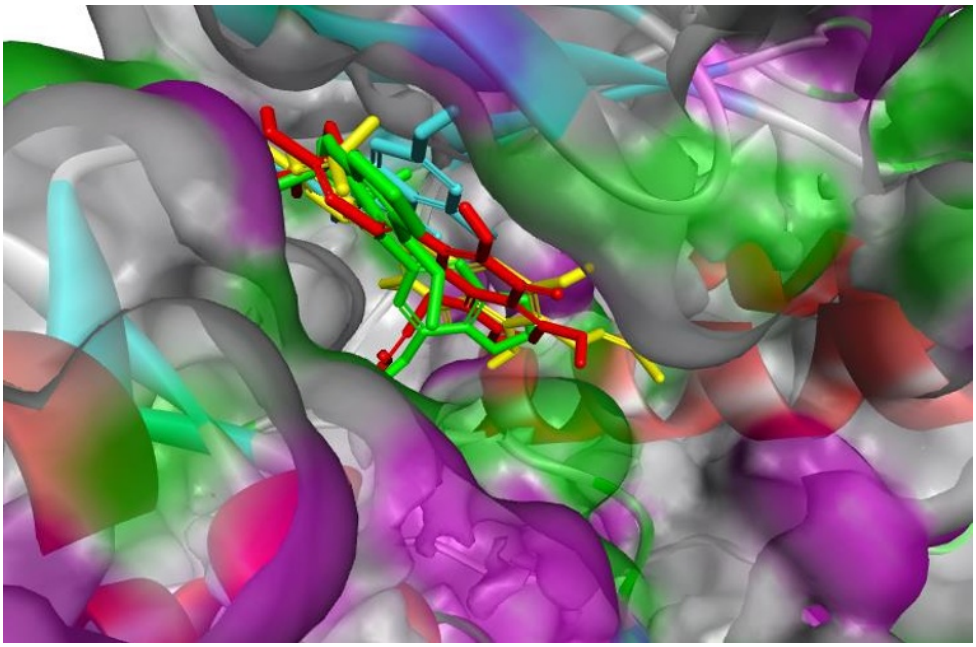

Figure 5. Top Three docked (Broussoflavonol F: Red; Glyasperin A; Yellow; and Sulabiroins A: Green) Compound and Norathyriol as Native Ligand (Blue) in the active site of MAPK1 (PDB ID: 3SA0).

Table 3. Docking Results

Compound	Binding Affinity (Kcal/Mol)	Contributing Binding Residues	
		Hydrogen Bond	**Hydrophobic Interaction**
Norathyriol (Control)	-7.2	Glu33, **Met108**, **Asp106**, **Gln105**	Gly32, Val39, Gly34, Lys54, Leu156, Ala52, Leu107, Ile84
Broussoflavonol F	-9	Asp167, Ala35, Lys114	Ile165, Leu156, **Gln105**, **Met108**, Val39, **Asp106**, Ile31, Ala52, Asp111, Ser153, Glu33, Gly34, Glu71, Lys54, Asn154
Glyasperin A	-9	Ala35, Glu71, **Met108**	Tyr36, Arg67, Lys54, Leu156, Ile84, **Asp106**, Ala52, Leu107, **Gln105**, Ile31, Lys114, Gly34, Val39, Asp167
Sulabiroins A	-8.8	-	Glu71, Asp167, Ser153, Asn154, Leu156, Val39, Ala52, Ile31, Lys114, Lys54

Bold : The same amino acids where references drugs and compounds interact with proteins and support from PDB ID literature source.

3.5 Molecular Dynamics

The potential compound selected as a result of molecular docking is reported to have better interaction stability (RMSD, RMSF, and Binding Energy) than Norathyriol, based on molecular dynamics results. The Root-Mean-Square Deviation (RMSD) value of the backbone structure shows that the MAPK1 complex with Sulabiroins A has better stability than the Native Ligand. Similarly, RMSD of the ligand structure also confirmed that Sulalabiroins A had better structural stability than Native Ligand. The average RMSF values obtained for Norathyriol (Control), Broussoflavonol F, Glyasperin A and Sulabiroins A were 1.51 Å, 1.65 Å and 1.48 Å respectively, indicating relatively stable behavior. The stability of the Active Sites distributed in each complex is reported to confirm the Complex Docking and Conformation results obtained from dynamic simulations. Based on the structural arrangement of the MAPK1 complex and its interactions with the active site residues of several selected compounds, it shows consistent stability below 2 Å during the simulation. Based on a comprehensive analysis of root mean square fluctuations (RMSF), it can be concluded that no statistically significant fluctuations were observed in the investigated system. Thus, the results of binding energy calculations found that Sulabiroins A, Glyasperin A and Broussoflavonol F had better stability than Norathyriol. This shows that in computational theory these three compounds have the potential to inhibit MAPK1 in the antiviral activity of COVID-19.

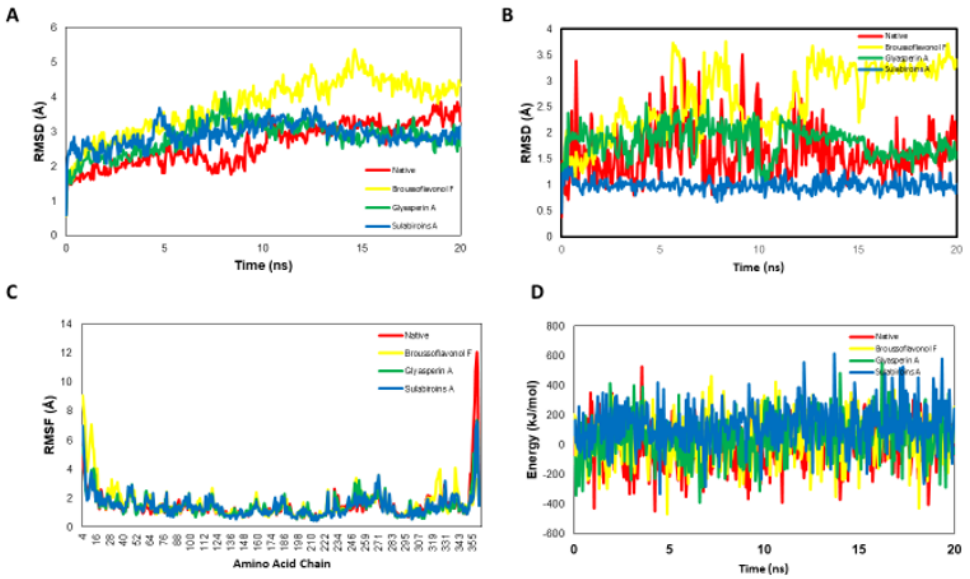

Fig. 6. Molecular dynamics simulation on the interaction of MAPK1 with selected compounds ; RMSD backbone (a), RMSD ligand (b), RMSF (c), and binding energy calculations (d).

Based on this research, the pathway mechanisms involved in propolis and COVID-19 have been studied from the collected literature, where the TNF signaling pathway can cause disruption in the localization of the zonula occludens-1 (ZO-1) junction and downregulation of ZO expression. -1, as well as other members of the claudin family in the lung, which functionally regulate the unblocking of TJs [67]. Through this pathway, Propolis can protect the alveolar endothelial/epithelial barrier by maintaining the integrity of the connections between cells, which ultimately reduces COVID-19 by improving lung ventilation function [68].

4 Conclusion

This research systematically analyzes the therapeutic targets, signaling pathways, and propolis mechanisms that can potentially be applied in the treatment of COVID-19 based on the Network Pharmacology approach and Molecular Docking and Molecular Dynamics verification. The therapeutic efficacy of propolis against COVID-19 is most likely mediated through the MAPK1 protein, where the compounds Broussoflavonol F, Glyasperin A, and Sulabiroins A from propolis were found to interact with MAPK1 through Molecular Docking and Molecular Dynamics. In addition, KEGG enrichment analysis illustrates that propolis can simultaneously play a role in various pathways in COVID-19, one of which is the Coronavirus disease pathway - COVID-19. Our research suggests that Broussoflavonol F, Glyasperin A, and Sulabiroins A may be helpful in COVID-19 therapy. These findings may provide a reference basis for clinical application and further exploration of the mechanism by which compounds in propolis affect COVID-19. Apart from that, MAPK1 as a potential therapeutic target in COVID-19 therapy has yet to be widely discussed so that this gene could be a suitable candidate. This needs to be done to provide a promising reference for future research.

Acknowledgement. We would like to express our deepest gratitude to the Bioinformatics Research Center (BRC INBIO) for facilitating research collaboration in the 2023 Internship Program.

References

1. K. A. A. K. Siregar & D.N.C. Hanifa, J. Public Heal. Trop. Coast. Reg. **4**, 28-34 (2021).
2. W, Wu. et al, Front. Endocrinol. (Lausanne). **14**, (2023).
3. J, Baj. et al, J. Clin. Med. **9**, 1753 (2020).
4. D. A. Berlin., R.M. Gulick & F.J. Martinez, N. Engl. J. Med. **383**, 2451-2460 (2020).
5. L. Hariri & C.C. Hardin, N. Engl. J. Med. **383**, 182–183 (2020).
6. M. N. Rivas., R.A. Porritt., M. H. Cheng., I. Bahar & M. Arditi, J. Allergy Clin. Immunol. **147**, 57–59 (2021).
7. A. A. Rabaan. et al, Ann. Clin. Microbiol. Antimicrob. **19**, 40 (2020).
8. Z. S. Lassi., R. Naseem., R. A. Salam., F. Siddiqui & J. K. Das, Int. J. Environ. Res. Public Health **18**, 988 (2021).
9. N. Mahroum. et al, Front. Immunol. **13**, (2022).
10. W. Dilokthornsakul., R. Kosiyaporn., R. Wuttipongwaragon & P. Dilokthornsakul, J. Integr. Med. **20**, 114–125 (2022)
11. C. A. Demeke., A. E. Woldeyohan & Z. D. Kifle, Metab. Open **12**, 100141 (2021).
12. P. Kashyap. et al, Molecules **27**, 6374 (2022).
13. R. Hossain. et al, Chin. Med. **17**, 100 (2022).
14. N. Yosri. et al, Foods **10**, 1776 (2021).
15. S. Ashraf. et al, Phyther. Res. **37**, 627–644 (2023).
16. G. Papadopoulou. et al, Pathogens **11**, 311 (2022).
17. D. I. Capraru. et al, Medicina (B. Aires). **59**, 877 (2023).
18. M. Rizzi. et al, Int. J. Mol. Sci. **24**, 7099 (2023).
19. W. P. Tsai. et al, J. Taiwan Inst. Chem. Eng. **147**, 104898 (2023).
20. S. Zheng., T. Xue., B. Wang., H. Guo & Q. Liu, Front. Bioinforma. **2**, (2022).
21. A. L. Hopkins, Nat. Chem. Biol. **4**, 682–690 (2008).
22. X. –D. Chu. et al, Transl. Cancer Res. **10**, 681–693 (2021).
23. X, Lai. et al, Front. Pharmacol. **11**, (2020).
24. Y. Zheng., S. Ji., X. Li & Q. Feng, PeerJ **10**, e13737 (2022).
25. D. –L. Ma., D. S. –H. Chan & C. –H. Leung, Chem. Sci. **2**, 1656–1665 (2011).
26. L. Pinzi & G. Rastelli, Int. J. Mol. Sci. **20**, 4331 (2019).
27. A. Vidal-Limon., J. E. Aguilar-Toala & A. M. Liceaga, J. Agric. Food Chem. **70**, 934–943 (2022).
28. R. S. Ibrahim & A. A. El-Banna, RSC Adv. **11**, 11610–11626 (2021).
29. A. H. Harisna. et al, Biochem. Biophys. Reports **26**, 100969 (2021).
30. L. K. Dewi. et al, Int. J. Appl. Pharm. **13**, 103–110 (2021).
31. M. Syaban. et al, J. Trop. Life Sci. **12**, 219–230 (2022).
32. A. C. Khayrani. et al, J. King Saud Univ. - Sci. **33**, 101297 (2021).
33. S. A. Hidayat., A. Susilo., K. U. A. Awwaly & M. Cahyati, J. Ilmu dan Teknol. Has. Ternak **17**, 123–134 (2022).
34. M. Sahlan. et al, J. King Saud Univ. - Sci. **33**, 101234 (2021).
35. J. F. Fatriansyah., R. K. Rizqillah., M. Y. Yandi., Fadilah & M. Sahlan, J. King Saud Univ. - Sci. **34**, 101707 (2022).
36. V. Kumar. et al, Phyther. Res. (2023) doi:10.1002/ptr.7717.
37. A. Daina., O. Michielin & V. Zoete, Sci. Rep. **7**, 42717 (2017).
38. M. Kuhn., C. V. Mering., M. Campillos., L. J. Jensen & P. Bork, Nucleic Acids Res.

36, D684–D688 (2007).
39. Z. –J. Yao. et al, J. Comput. Aided. Mol. Des. **30**, 413–424 (2016).
40. A. Daina., O. Michielin & V. Zoete, Nucleic Acids Res. **47**, W357–W364 (2019).
41. M. Safran. et al, in Practical Guide to Life Science Databases 27–56 (Springer Nature Singapore, 2021). doi:10.1007/978-981-16-5812-9_2.
42. M. Kanehisa., M. Furumichi., M. Tanabe., Y. Sato & K. Morishima, Nucleic Acids Res. **45**, D353–D361 (2017).
43. J. Chen. et all, Hematology **20**, 336–342 (2015).
44. Q. Pan., R. Zhou., M. Su & R. Li, Med. Sci. Monit. **25**, 4648–4654 (2019).
45. R. C. Gentleman. et al, Genome Biol. **5**, (2004).
46. L. Shang. et al, J. Ethnopharmacol. **302**, 115876 (2023).
47. L. Che. et al, Int. J. Chron. Obstruct. Pulmon. Dis. **Volume 16**, 2503–2513 (2021).
48. L. Shi. et al, Front. Genet. **13**, (2022).
49. D. Szklarczyk. et al, Nucleic Acids Res. **43**, D447–D452 (2015).
50. G. Stelzer. et al, Curr. Protoc. Bioinforma. **54**, (2016).
51. P. Shannon. et al, Genome Res. **13**, 2498–2504 (2003).
52. R. Gentleman., V. J. Carey., W. Huber., R. A. Irizarry & S. Dudoit, Bioinformatics and Computational Biology Solutions Using R and Bioconductor. (Springer New York, 2005). doi:10.1007/0-387-29362-0.
53. C. –H. Chin. et al, BMC Syst. Biol. **8**, S11 (2014).
54. H. Vaghasia., S. Sakaria., J. Prajapati., M. Saraf & R. M. Rawal, Comput. Biol. Med. **149**, 105994 (2022).
55. S. Dallakyan & A. J. Olson, in Chemical Biology 243–250 (Humana Press, 2015). doi:10.1007/978-1-4939-2269-7_19.
56. J. Li. et al, Cancer Res. **72**, 260–270 (2012).
57. S. K. Burley. et al, Nucleic Acids Res. **49**, D437–D451 (2021).
58. S. Kim. et al, Nucleic Acids Res. **51**, D1373–D1380 (2023).
59. J. L. Velázquez-Libera., F. Durán-Verdugo., A. Valdés-Jiménez., G. Núñez-Vivanco & J. Caballero, Bioinformatics **36**, 2912–2914 (2020).
60. X. Xinyi. et al, Digit. Chinese Med. **5**, 18–32 (2022).
61. A. C. Wallace., R. A. Laskowski & J. M. Thornton,"Protein Eng. Des. Sel. **8**, 127–134 (1995).
62. R. A. Laskowski & M. B. Swindells, J. Chem. Inf. Model. **51**, 2778–2786 (2011).
63. E. Krieger & G. Vriend, J. Comput. Chem. **36**, 996–1007 (2015).
64. J. A. Maier. et al, J. Chem. Theory Comput. **11**, 3696–3713 (2015).
65. B. R. Miller. et al, J. Chem. Theory Comput. **8**, 3314–3321 (2012).
66. V. Meylani. et al, Results Chem. **5**, 100721 (2023).
67. R. Al-Sadi, Front. Biosci. **Volume**, 2765 (2009).
68. X. Zhang. et al, Int. J. Med. Sci. **18**, 1866–1876 (2021).